

# The nature of super metal rich stars <sup>\*</sup>

## Detailed abundance analysis of 8 super-metal-rich star candidates

Sofia Feltzing<sup>1</sup> Guillermo Gonzalez<sup>2</sup>

<sup>1</sup> Lund Observatory, Box 43, SE-221 00 Lund, Sweden

<sup>2</sup> Astronomy Department, University of Washington, P. O. Box 351580, Seattle, WA 98195 USA

**Abstract.** We provide detailed abundance analyses of 8 candidate super-metal-rich stars. Five of them are confirmed to have  $[\text{Fe}/\text{H}] > 0.2$  dex, the generally-accepted limit for super-metal-richness. Furthermore, we derive abundances of several elements and find that the stars follow trends seen in previous studies of metal-rich stars. Ages are estimated from isochrones and velocities calculated. We find that there do exist very metal-rich stars that are older than 10 Gyr. This is contrary to what is found in several recent studies of the galactic age-metallicity relation. This is tentative evidence that there might not exist a one-to-one relation between age and metallicity for all stars. This is not surprising considering the current models of the independent evolution of the different galactic components. We also find that one star, HD 182572, could with  $\sim 75\%$  chance be a thick disk star with, for the thick disk, an extremely high metallicity at 0.34 dex. This star is, intriguingly, also somewhat enhanced in the  $\alpha$ -elements.

**Key words.** Stars: abundances, fundamental parameters, late-type, individual HD 10780, HD32147, HD99491, HD104304, HD121370, HD145675, HD196755, HD 182572, Galaxy: solar neighbourhood

### 1. Introduction

The very metal-rich dwarf stars in the solar neighbourhood have historically not attracted as much attention as the more metal-poor (solar like and halo stars) stars which tell us about the early phases of the chemical evolution of our galaxy. The properties of metal-rich stars are important when we try to interpret integrated spectra from metal-rich stellar populations, such as the Bulge and giant elliptical galaxies. A small group of so called super-metal-rich (SMR) stars have played a significant role in shaping the conceptions of such populations. Famous examples are the dwarf HD32147 (HR1614) and the giant  $\mu$  Leonis. In the review by Taylor (1996) - the latest paper in a long series started in the 1960s - SMR stars are discussed in great detail, in particular, the reality of extremely high  $[\text{Fe}/\text{H}]$ . Taylor found that no giant star fulfills the criteria for SMR-ness that he sets and only a handful of dwarf stars do, and that most of them are candidates rather than firm members in this class.  $\mu$  Leonis has, however, been studied by several groups using high-resolution spectroscopy, a recent example being Smith & Ruck (2000), who find that the star is indeed super-metal-rich with  $[\text{Fe}/\text{H}] = +0.29$ . Thus, the question of the reality of super-metal-rich giants

is still very much alive and each case has to be judged on its own.

The exact definition of super-metallicity has, as reviewed by Taylor (1996), varied. Spinrad & Taylor (1969) adopted +0.2 dex as the lower limit, based on the overall metallicity of the Hyades, which they found to be +0.2 dex. The metallicity for the Hyades has recently been revised (Taylor 1994 and Cayrel de Strobel 1997) to +0.1 dex. Even values as low as 0.0 dex have been quoted. This has resulted in classes of stars that sometimes are regarded as SMR and sometimes not. Taylor rectified this unsatisfactory situation by adopting the original +0.2 dex as the threshold on the grounds that no giant stars had been shown to have a metallicity higher than this value (but see Castro et al. 1997 and Smith & Ruck 2000). Taylor (1996) defines a star to be SMR if it has  $[\text{Fe}/\text{H}] > 0.20$  with 95% confidence. He also adopts  $[\text{Fe}/\text{H}]$ , i.e. the iron abundance, as the measure of “metallicity” rather than the more general  $[\text{Me}/\text{H}]$ . As an aside one may note that a second terminology is also in use - Very Strong-Lined (VSL) star. This term implies just that the star has strong lines and might therefore be a SMR candidate. This is a particularly useful term when working with low resolution spectra.

SMR stars have attracted more attention recently due to their possible connection with extra-solar planets, e.g. Gonzalez (2000 and references cited therein), Fuhrmann et

Send offprint requests to: Sofia Feltzing sofia@astro.lu.se

<sup>\*</sup> Based on observations obtained at the McDonald Observatory.

al. (1997, 1998). Gonzalez (2000) has shown that the solar-type parent stars of extra-solar planets are more metal-rich on average compared to the general field star population. In particular, the very short period systems are either above the SMR limit or near it. By comparing them to the SMR stars we may gain insight as to the relationship between planets in short-period orbits and the SMR-ness of the parent star.

A few other recent studies have targeted known SMR candidates and stars with high  $[\text{Me}/\text{H}]$  (as derived from photometry): Feltzing & Gustafsson (1998), Castro et al. (1997), and McWilliam & Rich (1994). In general the abundance ratios seem to continue the trends of the disk population. However, no detailed theoretical predictions for Galactic chemical evolution exists for  $[\text{Fe}/\text{H}] > 0.2$  dex, so the interpretation of the observed abundance trends for metal-rich stars is still pending.

The combination of abundance ratios with kinematical data may give us additional clues. For example, we can study stars on highly eccentric orbits which trace the evolution in the Galactic disk closer to the Galactic centre. Not much is known about these stars, but there are some very intriguing observations: Barbuy & Grenon (1990) found that dwarf stars on very eccentric orbits contained much more oxygen than what was expected from standard models of Galactic chemical evolution of the disk, and Edvardsson et al. (1993) found large spreads and “upturns” for certain elements, Na, Si, Ti, Al, for stars with  $0.0\text{dex} < [\text{Fe}/\text{H}] < 0.2$  dex. The trends for Na, Si and Ti were confirmed up to  $\sim 0.4$  dex by Feltzing & Gustafsson (1998). They concluded that the “upturn” in Na abundances relative to Fe is not due to a mixture of stars born at different distances from the Galactic centre.

In this paper we investigate, by means of detailed spectroscopic analyses, the metallicities as well as the abundance of several elements for 8 dwarf stars selected from the meticulous review of SMR candidates by Taylor (1996).

The paper is organized as follows: in Sect. 2 and 3 we detail the observations and the selection of program stars, as well as reductions and measurements; Sect. 4 discusses the detailed abundance analysis, Sect. 5 presents the abundances element by element, in Sect. 6 we derive ages for the stars and discuss the age-metallicity relation in the solar neighbourhood, Sect. 7 discusses the kinematics of the stars in our sample and which galactic component they belong to, Sect. 8 provides a short discussion of the SMR-planet connection and, finally, Sect. 9 summarizes our findings.

## 2. Selection of program stars and observations

Stars observable from the Northern Hemisphere were selected from Taylor’s 1996 list of candidate SMR dwarf and subgiant stars. Spectra were obtained with the Sandiford cassegrain echelle spectrograph (McCarthy et al. 1993) attached to the 2.1 m Struve telescope at McDonald Observatory during three runs: 1996 June, 1996 August

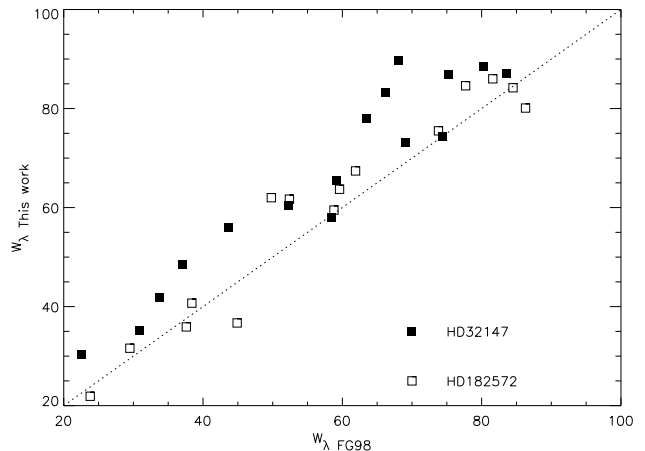


**Fig. 1.** Comparison of measurements of  $W_\lambda$  ( $\text{\AA}$ ) in this work and in Feltzing & Gustafsson (1998) for HD 32147 and HD 182572

and 1996 December. Exposure times were typically 5 minutes each, resulting in signal-to-noise (S/N) ratios per pixel averaging near 250. A spectrum of a Th-Ar lamp was obtained following each star spectrum, ensuring accurate wavelength calibration. The resolving power (measured on the Th-Ar emission line spectra) averages near  $R = 45,000$ .

## 3. Reductions and measurements

The spectra were reduced with the standard software available within the CCDRED and ECHELLE packages of NOAO IRAF<sup>2</sup>. The steps included bias subtraction, flat fielding, extraction of one-dimensional spectra, wavelength calibration, and continuum normalization. Additional details concerning the quality of the data resulting from the Sandiford spectrograph can be found in Gonzalez & Lambert (1996) and Gonzalez (1998).

Equivalent widths ( $W_\lambda$ ) were measured using the SPLOT task in IRAF. The lines were measured both by simply integrating the line and also by fitting a Gaussian to the line profile. Most lines were measured twice and some up to four times due to overlap of the spectral orders. As the final adopted value of  $W_\lambda$  we used the mean of the measurements. In these cases the measurement errors are typically no more than a few percent.

In Fig. 1 we compare the measured values of  $W_\lambda$  for HD 32147 and HD 182572 with those measured by Feltzing & Gustafsson (1998). For HD 182572 the agreement is good, while for HD 32147, our coolest star, we measure significantly larger  $W_\lambda$ . This difference is most likely due to the lower resolution used in this work. See also the two examples of stellar spectra shown in Fig. 3 from which it is clear that HD 32147, but also to some extent HD 145675,

<sup>2</sup> IRAF is distributed by National Optical Astronomy Observatories, operated by the Association of Universities for Research in Astronomy, Inc., under contract with the National Science Foundation, USA.

**Table 1.** Stellar parameters for the program stars. Magnitudes, colours and parallaxes are from the Hipparcos catalogue (ESA 1997). The spectral types are from the SIMBAD database. Effective temperatures, surface gravities, [Fe/H] and microturbulence parameters as determined in this study.

	Sp.T.	$V$	$B - V$	$\pi$ mas	$\sigma_\pi(\sigma_\pi/\pi)$	$T_{\text{eff}}$	$\log g$	[Fe/H]	$\xi_t$ km s $^{-1}$	
HD10780	HR511	K0V	5.63	0.804	100.24	0.68(0.007)	5300	4.13	-0.02	1.00
HD32147	HR1614	K3V	6.22	1.049	113.46	0.82(0.007)	4680	4.00	0.28	0.50
HD99491	HR4414A	K0IV	6.49	0.778	56.59	1.40(0.025)	5300	4.12	0.20	1.00
HD104304	HR4587	G9IV	5.54	0.760	77.48	0.80(0.01)	5400	4.12	0.16	1.15
HD121370	HR5235	G0IV	2.68	0.580	88.71	0.75(0.008)	6000	3.66	0.25	2.00
HD145675		K0V	6.61	0.877	55.11	0.59(0.011)	5300	4.50	0.47	1.00
HD182572	HR7373	G8IV	5.17	0.761	66.01	0.77(0.012)	5400	4.00	0.35	1.10
HD196755	HR7896	G5IV+	5.07	0.702	33.27	0.82(0.02)	5700	4.00	0.02	1.50
$\alpha$ Cen A <sup>1</sup>						5830	4.34	0.24	1.09	
$\alpha$ Cen B <sup>1</sup>						5225	4.51	0.23	1.00	

1.  $T_{\text{eff}}$ ,  $\log g$  and  $\xi_t$  from Neuforge-Verheeke & Magain (1997)

shows a much richer spectrum than the other stars. Since these stars are cool, there will naturally be more molecular lines and low-excitation atomic lines that will cause blending problems.

## 4. Analysis

We have performed a standard Local Thermodynamic Equilibrium (LTE) analysis, strictly differential with respect to the Sun, to derive chemical abundances from the measured values of  $W_\lambda$ . Spectrum synthesis was not employed in the present study.

### 4.1. Model atmospheres

To generate the model atmospheres we used the MARCS program, first described by Gustafsson et al. (1975). The program has been further developed and updated in order to handle the line blanketing of millions of absorption lines more accurately (Asplund et al. 1997). The following assumptions enter into the calculation of the models: the atmosphere is assumed to be plane-parallel and in hydrostatic equilibrium, the total flux (including mixing-length convection) is constant, the source function is described by the Planck function at the local temperature with a scattering term, the populations of different excitation levels and ionization stages are governed by LTE.

Since our analysis is strictly differential relative to the Sun, we have used a solar model atmosphere calculated with the same program as the stellar models – this in order to keep the analysis truly differential and thus in spite of the fact that the empirically derived Holweger-Müller model better reproduces the solar observed limb darkening (Blackwell et al. 1995).

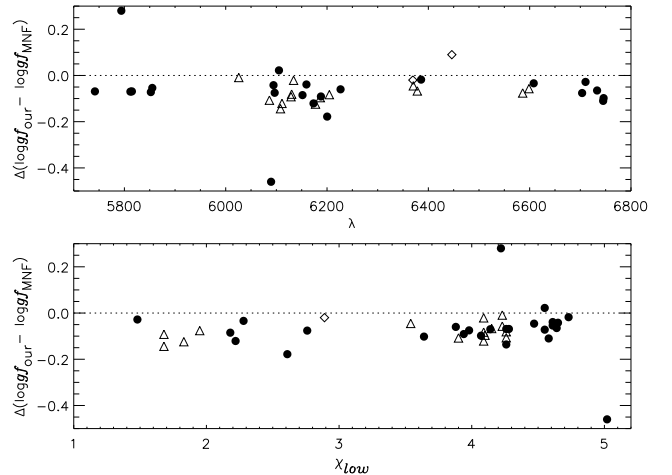


**Fig. 2.** Comparison of  $\log gf$ -values as derived in this study and in Neuforge-Verheeke & Magain (1997) study of  $\alpha$  Cen A and B. Fe I lines are denoted by  $\bullet$ , Fe II by  $\diamond$  and Ni I lines by  $\triangle$ .

### 4.2. Line data

Since we did not have observations of the solar spectrum for all of the lines available in the stellar spectra, we measured solar line strengths in the Kurucz et al. (1984) Solar Flux Atlas. The spectrum from the Flux Atlas was first degraded by binning and then convolved with a Gaussian profile to match the instrumental profile. To decide on the exact values of the convolution, we used three portions of a spectrum of reflected sunlight from Vesta. The Flux Atlas spectrum was convolved and then compared with the Vesta spectrum. The goodness of the fit was decided upon by inspection. The values of  $W_\lambda$  for all our lines were measured in the degraded spectrum. They were then used to determine the astrophysical  $\log gf$  values, Table 9.

We consider different line broadening mechanisms in our calculations; van der Waals damping, radiation damp-

ing, thermal Doppler broadening and broadening by microturbulence. The van der Waals broadening is calculated with the classical Unsöld formula. Enhancement factors to this value were compiled from the literature and are given in Table 9. For Fe we use values from Hannaford et al. (1992) and Holweger et al. (1991), for Ca, and for V from Neuforge (1992). For the remaining lines we use a value of 2.5, according to Mäcke et al. (1975). The values used for the enhancement factor do not, in general, influence the results, e.g. a change from 2.5 to 1.4 does not alter most abundances by more than 0.01 dex.

We have also compared our  $\log gf$ -values derived from the solar spectrum with those derived in a similar way, but using a Holweger-Müller solar model, by Neuforge-Verheecke and Magain (1997), Fig. 2. Our  $\log gf$ -values are 0.07 dex lower for Fe I lines and 0.04 dex lower for the Ni I lines than those derived by Neuforge-Verheecke and Magain (1997). Considering the different approaches to the derivation of the astrophysical  $\log gf$ -values we consider the agreement good. It is also reassuring that no trends are found either with wavelength or excitation potential, see Fig. 2.

#### 4.2.1. Selection of lines

Selecting stellar lines which are free from blends is crucial for deriving accurate elemental abundances. To account for telluric lines we simply over-plotted each stellar spectrum with a spectrum of a hot star observed during the same night as the stellar spectrum was taken and discarded lines that were contaminated. To avoid blends from unidentified photospheric lines the solar spectrum was carefully inspected and the line-list by Moore consulted.

Care in the selection of lines is also of importance for the determination of surface gravities by means of ionization equilibrium (i.e., abundances derived from Fe I and Fe II lines give the same iron abundance). We have inspected the shape of the Fe II lines in all the stars when a line is observed in more than two stars. This inspection led us to discard the lines at 6386.72 and 7449.33 Å, Fig. 3. A line at 5823.15 Å was also discarded, although only measured in two stars, since it gave anomalously high iron abundances and clearly suffered from blends. The line at 6416.91 Å gave rather high iron abundances in HD 10780, HD 32147 and HD 145675. From our spectra we could not, however, conclude that this line is compromised by a blend (see Fig. 3) and it was therefore kept in the analysis, but only in those stars where it did not diverge significantly. Our final selection of lines, as well as the parameters used in the abundance analysis, are given in Table 9.

#### 4.3. Fundamental parameters of model atmospheres

In order to construct the stellar model atmospheres we need the effective temperature, surface gravity, metallicity

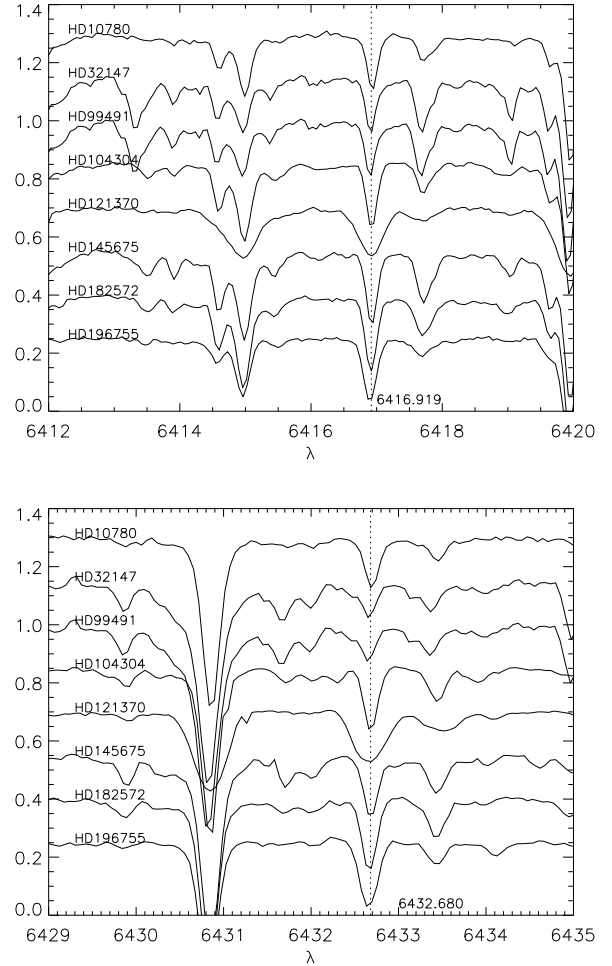


**Fig. 3.** Two portions of the stellar spectra, showing the regions around the two Fe II lines at 6416.91 and 6432.68 Å. The spectra have been arbitrarily displaced in intensity and also along the x-axis to the laboratory wavelengths. The positions of the Fe II lines are marked with dotted lines. Note the different scales on the x-axes.

and microturbulence for each star. These were all derived from the stellar spectra themselves.

**Effective temperature** Initial estimates of effective temperatures for the stars were determined using the photometric calibrations by Alonso et al. (1996). These estimates were iterated until excitation energy equilibrium was achieved. The plots from which the final temperatures were derived are shown in Fig. 4, and the final adopted temperatures are given in Table 1.

**Surface gravity** Surface gravities were determined by requiring ionization equilibrium for Fe abundances derived from Fe I and Fe II lines. We adjusted  $\log g$  until the iron abundance derived from Fe I and Fe II lines gave the same Fe abundance, compare Fig. 4.

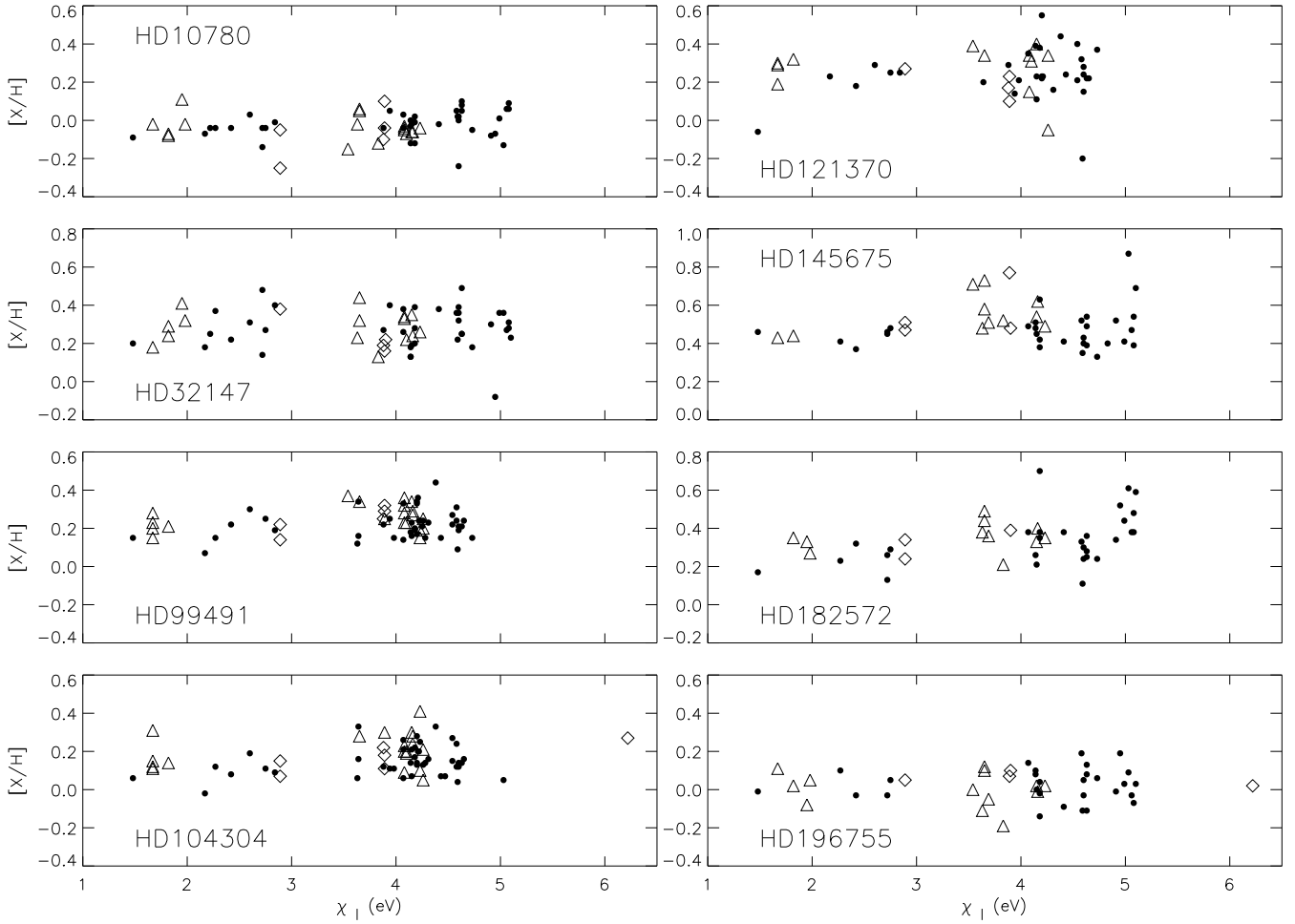


**Fig. 4.** Excitation equilibrium. Fe I lines are denoted by  $\bullet$ , Fe II by  $\diamond$  and Ni I lines by  $\triangle$ .  $[X/H]$  denote the abundance relative to solar as derived from Fe I, Fe II and Ni I lines, respectively. Note the different ranges on the y-axes.

**Metallicity** Our first estimates were taken from Taylor (1996). The  $[\text{Fe}/\text{H}]$  were iterated until the metallicity used in constructing the atmosphere and the derived  $[\text{Fe}/\text{H}]$  agreed.

**Microturbulence** The microturbulence parameter,  $\xi_t$ , which is introduced to account for unknown line broadening mechanisms, affects strong and weak absorption lines differently. For weak lines only the shape, and not the  $W_\lambda$  is affected, but for strong lines the line strength increases when  $\xi_t$  is increased. We use these trends to constrain the value of  $\xi_t$ .

We started with  $\xi_t = 1.00$  km/s and, after inspecting plots of  $[\text{Fe}/\text{H}]$  and  $[\text{Ni}/\text{H}]$  as a functions of  $W_\lambda/\lambda$  (reduced equivalent width), varied the value of  $\xi_t$  until all lines, weak and strong, yielded the same abundance. The final values used in the abundance analysis are given in Table 1.

#### 4.4. Comparison/verification with calibrations of *uvby* – $\beta$ photometry

As a further check of our final stellar parameters we have derived  $T_{\text{eff}}$ ,  $\log g$ , and  $[\text{Fe}/\text{H}]$  from the self-consistent calibration of  $T_{\text{eff}}$ ,  $\log g$  and  $[\text{Fe}/\text{H}]$  by Olsen (1984), Table 2. The agreement is in general good.

#### 4.5. Comparison with other studies

The stars in our study have been included in few, if any, abundance studies. However, HD 32147 and HD 182572 have been extensively studied. HD 32147 has been especially difficult to analyze, because it is a cool K dwarf star with strong lines. This is amply exemplified by the comparison of our  $W_\lambda$  measurements and abundances with those of Feltzing & Gustafsson (1998). In Table 3 we compare our results to theirs. As expected (from the comparison of  $W_\lambda$ ) the abundances for HD 32147 are larger in our study than in theirs. In this work we impose ionization equilibrium in order to derive the surface gravity of the star. This affects in particular the abundances derived

**Table 2.** Strömgren photometry and stellar parameters derived from the photometry thorough the calibration by Olsen (1984). References; O93=Olsen (1993), O94a=Olsen (1994a), O94b=Olsen (1994b), GO=Gronbech & Olsen(1997)

ID	b-y	$m_1$	$c_1$	ref.	Olsen (1984) $T_{\text{eff}}$	$\log g$
HD 10780	0.468	0.316	0.327	O93	5431	4.27
HD 32147	0.601	0.634	0.236	O94a	4614	4.57
HD 99491	0.484	0.335	0.362	O93	5347	4.12
HD 104304	0.469	0.313	0.345	O94a	5437	4.19
HD 121370	0.370	0.202	0.533	GO	6205	3.92
HD 145675	0.537	0.336	0.438	O93	4852	4.55
HD 182572	0.465	0.299	0.381	O93	5495	4.07
HD 196755	0.432	0.220	0.381	O94b	5642	3.98

**Table 3.** Comparison of results from this study with those of Feltzing & Gustafsson (1998), FG98, for HD 32147 and HD 182572

	HD 32147		HD 182572	
	This work	FG98	This work	FG98
Al I	0.48	0.25	0.55	0.53
Si I	0.36	0.48	0.49	0.51
Ca I		0.01		0.42
Sc II	–	0.49	0.36	0.36
Ti I	0.66	0.11	0.32	0.50
V I	0.95	-0.18		
Cr I	0.50	0.10	0.40	0.43
Fe I	0.28	0.22	0.34	0.42
Fe II	0.24	0.61	0.32	0.08
Co I	0.56	0.39	0.47	0.58
Ni I	0.29	0.57	0.36	0.46

from HD 32147, but also some of the species, i.e. Fe, Co and Ni, for HD 182572. For a discussion of stellar abundances in K dwarf stars, that for HD 32147 supersedes the

**Table 4.** Comparison for HD 121370 of results from this study with those of Edvardsson et al. (1993). The second line for Fe II give the iron abundance derived if the line at 6416.91 Å is excluded.

	This work	Edv.93
Na I	0.50	0.45
Si I	0.40	0.31
Ca I		0.23
Ti I	0.22	0.32
Fe I	0.24	0.19
Fe II	0.19	0.25
	0.22	
Ni I	0.31	0.30

current analysis, we refer the reader to Thorén & Feltzing (2000).

Gonzalez et al. (1999) found HD 145675 (14 Her) to have  $[\text{Fe}/\text{H}]$  of  $0.50 \pm 0.05$ , using a spectrum with nearly twice the resolution as ours. Nevertheless, it is in good agreement with our 0.47 dex estimate with a line-to-line scatter of 0.11 dex derived using 30 lines.

For HD 104304 François (1988) found  $[\text{Fe}/\text{H}] = 0.16$  and  $[\text{S}/\text{H}] = 0.59$ ; our estimate of  $[\text{Fe}/\text{H}] = 0.17$  is in excellent agreement. We derive an  $[\text{S}/\text{H}]$  value lower by 0.10 dex, but since our result is based on one fairly weak Si I line, we consider this to be a good agreement.

Morell et al. (1992) derived Fe and Th abundances for a group of stars in order to estimate their ages. For HD 182572 and HD 196755 they derived  $[\text{Fe}/\text{H}] = +0.3$  and  $+0.1$  dex, respectively. This is in reasonable agreement with our results.

Edvardsson et al. (1993) analyzed 189 dwarf and sub-giant stars with  $[\text{Fe}/\text{H}]$  up to  $+0.25$  dex, including HD 121370. The agreement between the two studies is very good, Table 4. Also, the stellar parameters agree well. These different comparisons give us confidence that our analysis is satisfactory.

#### 4.5.1. $\alpha$ Cen A and B

As a final test of our analysis method and its compatibility with the analysis procedures adopted by other groups, we derived elemental abundances for the stars in the nearby triple system  $\alpha$  Centauri from the equivalent widths published by Neuforge-Verheecke & Magain (1997). They observed the two stars (components A and B) with the CAT-telescope at La Silla with a resolution of 100,000 and a final  $S/N \sim 550$  and derived stellar abundances as well as stellar parameters self-consistently from the spectra. Using their published equivalent widths as well as their  $\log gf$  and damping parameters with our set of model atmospheres and programs, we derive almost the same abundances for all elements with lines that are not affected by hyperfine splitting, see Table 5. In fact for most of those elements taking the hyperfine structure in the line profile into account makes very little difference in the derived abundances. This is true in particular for Al.

For the A component we derive in general abundances 0.01 dex less than Neuforge-Verheecke & Magain (1997) and for the B component 0.02-0.03 dex higher abundances, see Table 5. Iron is however 0.01 dex lower for the B component. We find this level of agreement satisfactory considering that we use model atmospheres of slightly different construction.

## 5. Abundance results

The stellar abundances derived in this study are summarized in Table 6. We will discuss the abundance determination for each element separately. For some elements only one or a couple of lines have been used and the results are

**Table 5.** Comparison of abundances for  $\alpha$  Cen A and B derived by Neuforge-Verheeke & Magain (1997) and in this work using their equivalent widths and models as described in Sect. 4.5.1.

El.	# lines	$\alpha$ Cen A		# lines	$\alpha$ Cen B	
		This work [X/H] $\pm$ sc.	NVM97 [X/H] $\pm$ error		This work [X/H] $\pm$ sc.	NVM97 [X/H] $\pm$ error
O I	3	0.20 0.07	0.21 0.06			
Al I	1	0.23 0.00	0.24 0.04	1	0.27 0.00	0.24 0.05
Si I	3	0.26 0.02	0.27 0.03	3	0.30 0.00	0.27 0.04
Ca I	5	0.21 0.05	0.22 0.03	5	0.23 0.05	0.21 0.05
Sc II	1	0.35 0.00	0.25 0.05	1	0.36 0.00	0.26 0.04
Ti I	15	0.22 0.04	0.25 0.03	13	0.26 0.07	0.27 0.06
V I	4	0.22 0.04	0.23 0.05	4	0.40 0.07	0.32 0.08
Cr I	11	0.20 0.03	0.24 0.02	12	0.25 0.03	0.27 0.04
Cr II	2	0.25 0.02	0.26 0.03	1	0.29 0.00	0.26 0.09
Fe I	69	0.24 0.06	0.25 0.02	65	0.23 0.05	0.24 0.03
Fe II	4	0.25 0.03	0.25 0.02	4	0.27 0.04	0.25 0.02
Co I	3	0.29 0.04	0.28 0.04	3	0.39 0.02	0.26 0.04
Ni I	26	0.29 0.05	0.30 0.03	25	0.31 0.06	0.30 0.02
Y II	1	0.36 0.00	0.20 0.05	1	0.30 0.00	0.14 0.05
Eu II	1	0.17 0.00	0.15 0.05	1	0.16 0.00	0.14 0.05

**Table 6.** Derived elemental abundances for our program stars. The abundances are given in the format  $[X/H] = \log(X/H)_* - \log(X/H)_\odot$ , where X denotes the element in question. The ionization stages are also indicated. The line-to-line scatter is given for each star and element when more than one line is used in the abundance analysis. The error in the derived abundance due to line-to-line scatter is thus = line-to-line scatter /  $\sqrt{n_{lines}}$ , the number of lines used are given in parentheses. Oxygen abundances are given separately for the forbidden line at 630nm and the triplet at 777nm. No star has observations of both.

	HD10780	HD32147	HD99491	HD104304	HD121370	HD145675	HD182572	HD196755
C I	0.28	–	–	–	–	–	–	–
O <sub>1630</sub>	–	–	0.27	0.37	–	–	–	–
O <sub>1777</sub>	–	–	–	–	–	0.48 0.15 (3)	0.62 0.10 (3)	0.11 0.05 (3)
Na I	-0.03	0.64	0.34	0.37	0.50	–	–	–
Al I	-0.01 0.03 (3)	0.48 0.05 (3)	0.41	0.25	–	0.54 0.02 (3)	0.55 0.04(3)	0.02 0.05 (3)
Si I	0.03 0.05 (5)	0.36 0.15 (5)	0.35 0.10 (7)	0.27 0.08 (8)	0.40 0.14 (6)	0.61 0.07 (3)	0.49 0.18(6)	0.09 0.05 (4)
						0.52 0.19 (4)		
Ca I	0.13 0.10 (5)	–	0.18 0.08 (4)	0.15 0.07 (4)	0.11	0.21	0.28	-0.02 0.23 (2)
Si I	–	–	0.56	0.49	0.72	–	–	0.38
Sc I	–	–	0.10	0.11	–	–	–	–
Sc II	-0.12	0.36	–	0.32 0.13 (3)	0.11	0.66	0.36	0.11
Ti I	0.10 0.07 (2)	0.66 0.18 (2)	0.17 0.10 (13)	0.11 0.10 (12)	0.22 0.22 (3)	0.62 0.03 (2)	0.32 0.03 (3)	0.12 0.09 (3)
Cr I	0.01 0.15 (3)	0.50 0.12 (3)	0.19 0.11 (6)	0.14 0.09 (5)	0.22 0.04 (2)	0.42 0.04 (3)	0.40 0.01 (2)	-0.03 0.16 (2)
Cr II	–	–	0.35	0.26	–	–	–	–
Fe I	-0.02 0.07 (39)	0.28 0.11 (39)	0.22 0.08 (42)	0.15 0.08 (44)	0.24 0.14 (32)	0.47 0.11 (30)	0.34 0.14 (29)	0.02 0.09 (28)
Fe II	-0.11 0.10 (4)	0.24 0.10 (4)	0.24 0.07 (5)	0.17 0.08 (5)	0.19 0.07 (4)	0.49 0.02 (3)	0.32 0.08 (3)	0.06 0.03 (4)
						0.56 0.14 (4)		
Co I	-0.06 0.06 (4)	0.56 0.19 (4)	0.26 0.08 (5)	0.04 0.54 (6)	0.32	0.81 0.11 (4)	0.47 0.07 (3)	0.27
Ni I	-0.03 0.06 (17)	0.29 0.08 (15)	0.26 0.07 (20)	0.20 0.09 (19)	0.31 0.16 (13)	0.55 0.10 (11)	0.36 0.08 (18)	0.00 0.09 (13)

therefore more tentative than firm. The number of lines used for each element are also indicated in the table.

dex. Thus, the error in Fe abundances is negligible in the error budget for the abundance ratios.

**Iron abundances** Iron abundances are derived from a large number of lines, 28 to 44 lines per star, which means that the errors in the mean are very small, typically less 0.02

In Table 7 we compare the iron abundances in this study and those quoted by Taylor (1996). For HD 32147, HD 99491, HD 121370, HD 145675, and HD 182572 their SMR status is confirmed. HD 104304 is a marginal case

**Table 7.** Comparison of  $[\text{Fe}/\text{H}]$  from Taylor (1996) and this work. We also give, in column 3 and 4, the VSL and SMR status for the stars according to Taylor (1996).

ID	VSL	SMR	$[\text{Fe}/\text{H}]$ (Taylor)	$[\text{Fe}/\text{H}]$ This work
HD 10780	no		0.396	-0.02
HD 32147	yes		> 0.1	0.28
HD 99491	marg		0.115	0.20
HD 104304	marg		0.326	0.16
HD 121370		95%	0.305	0.25
HD 145675	marg	98%	0.38	0.47
HD 182572		98%	>0.341	0.35
HD 196755			0.500	0.02

and HD 10780 and HD 196755 are shown to not be SMR stars.

**Oxygen** The forbidden O I line at 6300 Å was only measured in two stars, HD 99491 and HD 104304; they have  $[\text{O}/\text{Fe}]$  of 0.05 and -0.17 dex, respectively. The errors in the O abundances are dominated by the measurement error for the [O I] line. Our spectra have S/N of  $\sim 250$ , which translates into an uncertainty of  $\sim 0.15$  dex in  $[\text{O}/\text{Fe}]$ . Thus, our observed  $[\text{O}/\text{Fe}]$  are well within this scatter, and our data follow the trends found in Nissen & Edvardsson (1992) and Feltzing & Gustafsson (1998).

Three of our stars have useful observations of the triplet lines around 777 nm. For those three stars we get  $[\text{O}/\text{Fe}] = 0.01, 0.28,$  and  $0.09$  dex respectively. Line-to-line scatter is 0.1 dex or less for these stars which means that formal errors are less than 0.1 dex for all three stars. These oxygen abundances should be fairly reliable as we are dealing with stars that are similar to the Sun and our study is differential. Edvardsson et al. (1993) found a good correlation between oxygen abundances derived from the forbidden line and those derived from the triplet. Note, however, that Feltzing & Gustafsson (1998) found no such correlation for their very metal-rich sample. Thus, in conclusion, the  $[\text{O}/\text{Fe}]$  for HD 196755 derived from the triplet should be robust while the  $[\text{O}/\text{Fe}]$  for HD 145675 and HD 182572 are more uncertain in term of possible NLTE effects.

**Sodium** Only one Na I line was available for analysis in our spectra, but it has been widely used in other abundance studies. Therefore, we are confident that it is giving us reliable Na abundances.

**Aluminum** Aluminum shows a somewhat puzzling behaviour. Both Edvardsson et al. (1993) and Feltzing & Gustafsson (1998) found  $[\text{Al}/\text{Fe}]$  to be solar for all stars with  $[\text{Fe}/\text{H}] > 0.0$  dex. However, three of our stars show

unexpectedly high  $[\text{Al}/\text{Fe}]$  abundances. The line-to-line scatter is small for all stars with all three lines measured.

**Silicon** A flat distribution with some internal scatter is found. The line-to-line scatter is, as in Feltzing & Gustafsson (1998), on the larger side for the number of lines used.

**Calcium** For three stars we observe several lines of Ca I. These stars all show  $[\text{Ca}/\text{Fe}]$  close to the solar value, as expected. For the other stars only one or two lines were available and the results are therefore uncertain.

**Sulfur** Our linelist contains 2 S I lines, however, for those stars where we could determine S abundances only one line was available in each star. Our abundances are therefore uncertain. We note that  $[\text{S}/\text{Fe}]$  appears somewhat high.

**Scandium** Sc abundances were derived from both Sc I and Sc II lines. The  $[\text{Sc}/\text{Fe}]$  values fall within the range expected from Feltzing & Gustafsson (1998) and the trend in our  $[\text{Sc}/\text{Fe}]$  data is flat at around 0.1-0.15 dex. We note though that our most metal rich stars are overabundant in Sc in contrast with Feltzing & Gustafsson (1998) which show a tendency for the most metal-rich stars to be underabundant.

**Titanium** An overall flat trend is found for our stars in accordance with previous studies, i.e. Feltzing & Gustafsson (1998). HD 32147 stands out with an extremely high Ti abundance, perhaps indicative of an underestimated temperature (see Thorén & Feltzing 2000).

**Chromium** The behaviour is the same as found by Feltzing & Gustafsson (1998), except for HD 32147. Essentially,  $[\text{Cr}/\text{Fe}]$  has a flat trend above solar metallicity.

**Cobalt** We find a large scatter in the  $[\text{Co}/\text{Fe}]$  abundances. The origin of this large scatter is not entirely clear, but it is accompanied by a large line-to-line scatter as well, and thus the reason may be sought among the selection of stellar lines.

**Nickel** A large number of Ni I lines were used, both to determine the effective temperature as well as the Ni abundances. All our stars have virtually solar  $[\text{Ni}/\text{Fe}]$  in agreement with Edvardsson et al. (1993) and Feltzing & Gustafsson (1998) for stars in this  $[\text{Fe}/\text{H}]$  range. Interestingly, we find that our most metal-rich star, HD 145675, shows a slightly enhanced  $[\text{Ni}/\text{Fe}]$ . Tentative enhancements of Ni in the most metal-rich stars can be found also in the studies by Feltzing & Gustafsson (1998) and Thorén & Feltzing (2000). All three studies adopted different techniques for derivation of stellar parameters, and



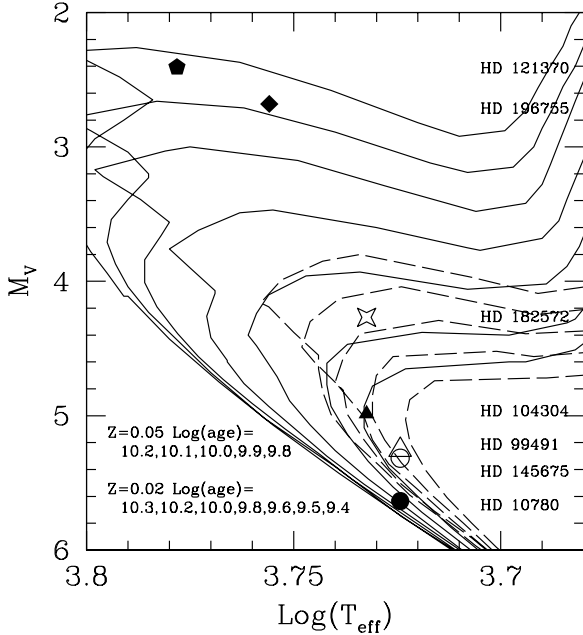


**Fig. 5.** Diagram used to estimate ages for our program stars. Isochrones are from Bertelli et al. (1994). Full curves correspond to  $Z=0.02$ , and the dashed curves to  $Z=0.05$  isochrones, respectively. Filled symbols denote stars with  $[\text{Fe}/\text{H}] \leq 0.20$  dex and open circles stars with  $[\text{Fe}/\text{H}] > 0.20$  dex. HD 32147 is too cool to show on the diagram.

thus the result seems to be significant. However, further investigations should be undertaken.

## 6. Ages of SMR stars and the Age-metallicity relation

An age-metallicity relation among dwarf stars in the solar neighbourhood is a key observable that models of galactic chemical evolution must match. The most important recent studies include Edvardsson et al. (1993), Carraro et al. (1998), and Rocha-Pinto et al. (2000). The first two studies use the same  $[\text{Fe}/\text{H}]$ , as derived in Edvardsson et al. (1993) from detailed abundance analysis. Carraro et al. (1998) make use of the age determinations done for Edvardsson et al. (1993) sample post Hipparcos (Ng & Bertelli 1998). Essentially, their data show a declining trend such that more metal-poor stars are older. However, the intrinsic scatter appears large in both age and  $[\text{Fe}/\text{H}]$  and a unique age-metallicity relation may not be present. The study by Rocha-Pinto et al. (2000) used a different technique to determine ages, chromospheric activity. They arrive at the conclusion that there exists a unique age-metallicity relation in the solar neighbourhood. The scatter in both age and metallicity are found to be small for all ages and metallicities (see their Fig. 13).

SMR stars are rare and therefore none of the studies discussed contain large numbers of them, in fact e.g. the Edvardsson et al. (1993) sample was selected with an upper limit in metallicity near 0.2 dex. Such a bias is not

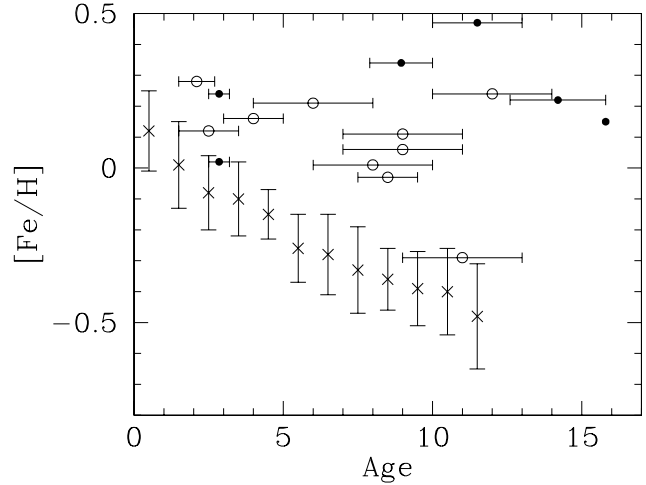


**Fig. 6.** A comparison of our isochrone ages with the general age-metallicity relation derived by Rocha-Pinto et al. (2000).  $\bullet$  refer to stars in this study,  $\circ$  to stars from Gonzalez, see Table 8.  $\times$  refers to the age-metallicity relation from Rocha-Pinto et al. where the error bars give the  $1\sigma$  scatter around the mean  $[\text{Fe}/\text{H}]$  for each age bin.

present in the Rocha-Pinto et al. (2000) sample, and they have a few stars of up to  $\sim 0.3$  dex (their Fig. 13). It is therefore valuable to derive ages for our small sample of stars and compare them to that of the general age-metallicity relations found in previous studies.

We have simply estimated the ages of the stars by plotting them in the  $M_V - T_{eff}$  plane and using the Bertelli et al. (1994) isochrones, Fig. 5. The ages were estimated by eye. The correct isochrones were chosen depending on the  $[\text{Fe}/\text{H}]$  for each star as derived in this study. In order to see if the age-metallicity relation appears unique also for the most metal-rich stars, we compare our data and the ages from the several papers by Gonzalez and co-workers, see Table 8, with the age-metallicity relation found in Rocha-Pinto et al. (2000) in Figure 6.

A possible error source in the age determination of SMR stars is the presence of planets. Gonzalez (1998) noted that if one or several planets have been engulfed by a star, then its  $[\text{Fe}/\text{H}]$  may increase by up to around 0.10 dex. If this has happened, then the abundances and age for a polluted star will no longer represent its true age and abundances. However, such a change in metallicity would still not turn a  $\sim 10$  Gyr star into a star of only a few Gyr, as required to fit into a general age-metallicity relation.

We note that our sample is not complete or in any other way well-defined. However, it proves also that there exist stars that are both very old and at the same time very metal-rich, also taking the errors in the ages into account. This casts doubts on the possibility of defining a one-to-one relation between age and metallicity among the solar neighbourhood stars.

**Table 8.** Velocity data and age determinations. The top half of the table contains the stars in this study and the lower section stars from Gonzalez (1999) and Gonzalez & Laws (2000). Age estimates, using isochrones, from this study are given in column 6 top half. The age estimates for the stars in the second section are also based on the Bertelli et al. (1994) stellar isochrones, with typical uncertainties of 1 to 2 Gyrs. In column 7 we reproduce the Ca II activity index ages from Gonzalez (1998). In the last column we give [Fe/H] as determined in this study or from Gonzalez (1999) and Gonzalez & Laws (2000).

ID	Name	$U_{\text{LSR}}$ (km/s)	$V_{\text{LSR}}$ (km/s)	$W_{\text{LSR}}$ (km/s)	Age (isochrones) (Gyr)	Age (Ca II) (Gyr)	[Fe/H]
HD10780		-14.8	-11.3	1.6	–		-0.02
HD32147		10.7	-51.8	-6.3	–		0.28
HD99491		-49.8	-4.1	-8.7	12.6 – 15.8		0.22
HD104304		31.6	-10.2	-9.2	$\leq 15.8$		0.15
HD121370		19.2	-12.0	4.6	2.5 – 3.2		0.24
HD145675	14 Her	35.6	-2.0	-2.9	10 – 13.0		0.47
HD182572		-106.7	-25.2	-13.5	7.9 – 10.0		0.34
HD196755		-48.1	29.	-11.7	2.5 – 3.2		0.02
HD9826	$\nu$ And	4.3	-34.1	0.6	2.7		0.12
HD75732	$\rho^1$ Cnc	-27.3	-13.2	-0.9		5	0.45
HD75289		31.1	-12.4	-14.5	2.1		0.28
HD95128	47 UMa	-14.7	2.6	8.8	6.3	7	0.01
HD117176	70 Vir	23.2	-46.9	3.4	8	9	-0.03
HD120136	$\tau$ Boo	-23.5	-13.8	0.3	1		0.32
HD143761	$\rho$ CrB	64.1	-30.7	28.5	12.3		-0.29
HD186408	16 Cyg A	27.6	-23.6	7.2	9.0		0.11
HD186427	16 Cyg B	27.1	-24.7	5.4	9.0	7	0.06
HD187123		11.6	-10.6	-36.4	5.5		0.16
HD217014	51 Peg	-5.6	-24.2	22.3	6.0	10	0.21
HD210277		12.4	-46.8	3.0	8.5		0.24

## 7. Velocity data

Spatial velocity data were calculated using the Hipparcos parallaxes and proper motions. Radial velocities were taken from Barbier-Brossat et al. (1994). For our stars the uncertainties in the parallaxes are small, less than 3% of the parallax, Table 1. Data were also obtained for the stars from the Gonzalez (1999) compilation. The velocities are presented in Table 8. Note that we here quote the velocities relative to the local standard of rest (LSR) and Gonzalez (1999) quoted velocities relative to the sun.

From Table 8 we see that all the stars have  $W$ -velocities well below the  $\sigma_W$  of the general population of stars with similar  $B-V$ . Fig. 5 in Dehnen & Binney (1998) illustrates how  $\sigma_{U,V,W}$  varies with  $B-V$ . Also, most of the stars in Table 8 have both  $V$  and  $U$ -velocities well below 1  $\sigma$  for the general population. We have quantified this by calculating the probabilities that any one of our stars belongs to either the thin or the thick disk by using a model where 94% of the solar neighbourhood stars belong to a thin disk with  $\sigma_U = 35$ ,  $\sigma_V = 25$ , and  $\sigma_W = 17$  km/s and the remaining 6% to the thick disk with  $\sigma_U = 70$ ,  $\sigma_V = 50$ , and  $\sigma_W = 34$  km/s. Only one of our stars, HD 182572, has a probability that it belongs to the thick disk larger than that it should belong to the thin. We estimate that, given the galactic model, this star has 75% chance

of belonging to the thick disk. Thus, we conclude that our SMR and planet-bearing stars samples the thin disk.

Fuhrmann (1998) found that stars with thick disk kinematics were enhanced in [Mg/Fe] as compared to thin disk stars at the same metallicity. We have not measured Mg lines in our spectra. We did, however, measure Si, and our abundance result for HD 182572 gives [Si/Fe] =  $0.16 \pm 0.09$ . Compared with the general trend of [Si/Fe] for metal-rich stars in Feltzing & Gustafsson (1998), this is above the mean; however, their data exhibit a large scatter. We have also determined Ca abundances for this star, however, only one line was available. This line seems to give fairly low Ca abundances in all of the stars with more than two lines observed and may thus be underestimating the true Ca abundance in this star. Note that it is not inconsistent that we also find thin disk stars with the same Si abundance as, if HD 182572 is a thick disk star, then it might be showing us the abundance trend after the decline in [X/Fe], where X is either O or an  $\alpha$ -element, sets in due to increasing relative contribution of SNIa.

## 8. SMR - planet connection

Several of the nearby SMR star candidates listed by Taylor (1996; Table 4) have been found to harbour planets. In particular, the planet-bearing stars HD 75732, HD 145675,

and HD 217014 are included in Taylor's list of 29 SMR class IV-V star candidates. Not all the stars in his list have been searched for planets as of yet, so the fraction of SMR star candidates with planets may increase. Butler et al. (2000) provide independent confirming evidence for a preponderance of planets among metal-rich stars; they note that of their 600 Keck targets, half of which are metal-poor, 2 planets have been found around metal-poor stars and 10 around metal-rich stars. Also, several planet-bearing stars not in Taylor's list have recently been found to be likely SMR stars. Examples in this group include HD 120136, HD 217107, and HD 210277 (Gonzalez 2000). It appears that the Doppler planet search method is also an efficient detector of new SMR star candidates!

Gonzalez et al. (1999) suggested that BD  $-10^{\circ}3166$  be searched for planets on the basis of its similarity to HD 75732 and HD 145675 (similar  $T_{\text{eff}}$  and  $[\text{Fe}/\text{H}]$ ). Butler et al. (2000) reported on the detection of a planet around BD  $-10^{\circ}3166$ , which they had placed on their monitoring program as a result of Gonzalez et al.'s suggestion. Another star, HD 89744, was suggested to Geoff Marcy as a planet-bearing candidate by one of us (G.G.) on the basis of its high  $[\text{Fe}/\text{H}]$  and low  $[\text{C}/\text{Fe}]$ . Sylvain et al. (2000) announced the discovery of a planet around this star (note: they began observing this star about 2 years before Gonzalez's prediction). The successful prediction of the presence of planets around two stars provides strong independent confirming evidence of the planet - SMR star connection. The low  $[\text{C}/\text{Fe}]$  values seen among stars with planets is the first convincing evidence of a trend with abundance ratios. The physical significance of this trend is not yet known.

## 9. Conclusions

We have presented detailed abundance analyses at high resolution for 8 possible SMR dwarf stars and subgiants. Four of these stars have previously been studied at high resolution; our results in general agree well with them. For the remaining four stars this is, to the best of our knowledge, the first study of this sort.

We find in particular that:

- HD32147, HD99491, HD121370, HD145675, HD182572 all have  $[\text{Fe}/\text{H}] \geq 0.2$  dex, the lower limit for super metal rich status as defined by Taylor (1996)
- HD104304 presents a marginal case
- HD10780 and HD196755 are found to have solar iron abundances and are thus not SMR stars
- some metal-rich, and in particular SMR, stars are old, showing that the large scatter in  $[\text{Fe}/\text{H}]$  at a given age among nearby solar type stars exists at all ages and that a one-to-one relation between age and metallicity among the solar neighbourhood stars may not exist for all metallicities.

- that metal-rich stars are mainly confined to the galactic plane, however, one star in our sample appears to be a thick disk candidate of extremely high metallicity
- there exists a correlation between SMR-ness and the presence of planets

Further investigations should be undertaken to prove the possibility that  $[\text{Ni}/\text{Fe}]$  is starting to increase at the highest metallicities as well as the very real possibility that there exists extreme thick disk stars with very high metallicities. In particular,  $\alpha$ -element abundances should be carefully studied for such candidates.

*Acknowledgements.* SF acknowledges financial support from the Swedish Natural Research Council under their post-doc program. GG acknowledges financial support from the Kennilworth Fund of the New York Community Trust.

Johan Holmberg at Lund Observatory is thanked for providing stellar velocities.

## References

- Alonso, A., Arribas, S., Martinez-Roger, C., 1996 A&A 313, 873
- Asplund, M., Gustafsson, B., Kiselman, D., Eriksson, K., 1997, A&A 318, 521
- Barbier-Brossat, M., Petit, M., Figon, P., 1994, A&AS 108, 603
- Barbuy, B., Grenon, M., 1990, in ESO/CTIO Workshop on Bulges of Galaxies, p. 83
- Bertelli, G., Bressan, A., Chiosi, C., Fagotto, F., Nasi, E., 1994, A&AS 106, 275
- Blackwell, D.E., Lynas-Gray, A.E., Smith, G., 1995, A&A 296, 217
- Butler, R.P., Vogt, S.S., Marcy, G.W., et al., 2000, ApJ, submitted
- Carraro, G., Ng, Y.K., Protinari, L., 1998, MNRAS 296, 1045
- Castro, S., Rich, R.M., Grenon, M., Barbuy, B., McCarthy, J.K., 1997, AJ 114, 376
- Cayrel de Strobel, G., Soubiran, C., Friel, E.D., Ralite, N., François, P., 1997, A&AS 124, 299
- Dehnen, W., Binney, J.J., 1998, MNRAS 298, 387
- Edvardsson, B., Andersen, J., Gustafsson, B., Lambert, D.L., Nissen, P.E., Tomkin, J., 1993, A&A 275, 101
- ESA, 1997, The Hipparcos and Tycho Catalogues, ESA SP-1200
- Feltzing, S., Gustafsson, B., 1998, A&AS 129, 237
- Feltzing, S., Holmberg, J., 2000, A&A, 357, 153
- François, P., 1988, A&A 195, 226
- Fuhrmann, K., 1998, A&A 338, 161
- Fuhrmann, K., Pfeiffer, M.C., Bernkopf, J., 1997, A&A 326, 1081
- Fuhrmann, K., Pfeiffer, M.C., Bernkopf, J., 1998, A&A 336, 942
- Gonzalez, G., 1998, A&A 334, 221
- Gonzalez, G., 1999, MNRAS 308, 447
- Gonzalez, G., 2000, In: Garzon F., Eiroa C., de Winter D., Mahoney T.J. (eds.) Disks, Planetesimals, and Planets, ASP Conference Series, in press
- Gonzalez, G., Lambert, D.L., 1996, AJ 111, 424
- Gonzalez, G., Laws, C., 2000, AJ 119, 390
- Gonzalez, G., Wallerstein, G., Saar, S.H., 1999, ApJ 511, L111
- Gronbeck, S.L., Olsen, E.H., 1977, A&AS 27, 443

Gustafsson, B., Bell, R.A., Eriksson, K., Nordlund, Å., 1975, A&A 42, 407  
 Hannaford, P., Lowe, R.M., Grevesse, N., Noels, A., 1992, A&A 259, 301  
 Holweger, H., Bard, A., Kock, A., Kock, M., 1991, A&A 249, 545  
 Kurucz, R.L., Furenlid, I., Brault, J., Testerman, L., 1984, Solar Flux Atlas from 296 to 1300 nm, National Solar Observatory  
 Mäckle, R., Holweger, H., Griffin, R., Griffin, R., 1975, A&A 38, 239  
 McCarthy, J.K., Sandiford, B. A., Boyd, D., Booth, J., 1993, PASP 105, 881  
 McWilliam, A., Rich, M., 1994, ApJS 91, 749  
 Morell, O., Källander, D., Buthcer, H.R., 1992, A&A 259, 543  
 Neuforge, C., 1992, in Origin and Evolution of Elements, eds. Prantzos, N., Vangioni-Flam, E., Cassé, M., 63  
 Neuforge-Verheecke, C., Magain, P., 1997, A&A 328, 261  
 Ng, Y.K., Bertelli, G., 1998, A&A 329, 943  
 Nissen, P.E., Edvarsson, B., 1992, A&A 261, 255  
 Olsen, E.H., 1984, A&AS 57, 443O  
 Olsen, E.H., 1993, A&AS 102, 89  
 Olsen, E.H., 1994a, A&AS 104, 429  
 Olsen, E.H., 1994b, A&AS 106, 257  
 Rocha-Pinto, H.J., Maciel, W.J., Scalo, J., Flynn, C., 2000, A&A, 358, 850  
 Smith, G., Ruck, M. J., 2000, A&A 356, 570  
 Spinrad, H., Taylor, B.J., 1969, ApJ 157, 1279  
 Sylvain, G.K., Brown, T.M., Fischer, D.A., Nisenson, P., Noyes, R.W., 2000, ApJ 533, L147  
 Taylor, B.J., 1996, ApJS 102, 105  
 Taylor, B.J., 1994, PASP 106, 600  
 Thorén, P., 2000, A&A Letters, 358, L21  
 Thorén, P., Feltzing, S., A&A, 2000, accepted for publication

**Table .1.** Line data.

$\lambda$ [Å]	$\chi_l$ [eV]	$\log gf$	$\delta\Gamma_6$	$\Gamma_{\text{rad}}$ [s <sup>-1</sup> ]	Note
<b>C I; <math>\log \epsilon_{\odot} = 8.56</math></b>					
6587.61	8.53	-1.246	2.50	1.00e+08	
<b>O I; <math>\log \epsilon_{\odot} = 8.93</math></b>					
6300.310	0.00	-9.75	2.50	1.00e+08	
7771.95	9.14	0.26	2.50	1.00e+08	
7774.17	9.14	0.12	2.50	1.00e+08	
7775.35	9.14	-0.11	2.50	1.00e+08	
<b>Na I; <math>\log \epsilon_{\odot} = 6.33</math></b>					
6154.23	2.10	-1.58	2.10	7.08e+07	
<b>Al I; <math>\log \epsilon_{\odot} = 6.47</math></b>					
6698.67	3.143	-1.89	2.50	3.02e+08	
7835.30	4.022	-0.78	2.50	7.94e+07	
7836.13	4.022	-0.60	2.50	7.94e+07	
<b>Si I; <math>\log \epsilon_{\odot} = 7.55</math></b>					
5622.22	4.930	-2.95	2.50	1.95e+08	
5665.55	4.920	-2.02	2.50	1.95e+08	
5793.07	4.930	-1.95	2.50	1.95e+08	
6125.02	5.614	-1.55	2.50	1.00e+08	
6142.48	5.619	-1.50	2.50	1.00e+08	
6155.69	5.619	-2.43	2.50	1.00e+08	
6237.31	5.614	-1.15	2.50	1.00e+08	
6721.84	5.863	-1.16	2.50	1.00e+08	
6741.62	5.984	-1.63	2.50	2.69e+07	
6848.58	5.863	-1.65	2.50	1.00e+08	
7455.37	5.964	-2.00	2.50	1.00e+08	
7760.62	6.206	-1.36	2.50	1.00e+08	
7799.99	6.181	-0.77	2.50	1.00e+08	
<b>S I; <math>\log \epsilon_{\odot} = 7.21</math></b>					
6743.531	7.866	-0.84	2.50	3.80e+07	
6757.171	7.870	-0.53	2.50	3.89e+07	
<b>Ca I; <math>\log \epsilon_{\odot} = 6.36</math></b>					
5512.980	2.933	-0.66	2.50	2.80e+08	
5581.965	2.523	-0.87	2.50	7.13e+07	
5867.562	2.933	-1.61	2.50	2.62e+08	
6166.439	2.521	-1.22	2.50	1.86e+07	
6169.042	2.523	-0.90	2.50	1.86e+07	
6169.563	2.526	-0.67	2.50	1.88e+07	
6455.598	2.523	-1.48	2.50	4.64e+07	
6464.673	2.526	-2.36	2.50	4.64e+07	
6471.662	2.526	-0.98	2.50	4.42e+07	
<b>Sc I; <math>\log \epsilon_{\odot} = 3.10</math></b>					
5484.626	1.851	0.37	1.50	1.46e+08	
<b>Sc II; <math>\log \epsilon_{\odot} = 3.10</math></b>					
5526.790	1.768	0.09	1.50	2.16e+08	
6300.698	1.507	-2.01	1.50	2.31e+08	
6604.601	1.357	-1.16	1.50	1.46e+08	
<b>Ti I; <math>\log \epsilon_{\odot} = 4.99</math></b>					
5490.148	1.460	-0.98	2.50	1.43e+08	
5739.469	2.249	-0.78	2.50	6.60e+07	
5739.978	2.236	-0.74	2.50	6.53e+07	
5823.686	2.267	-1.05	2.50	6.53e+07	
5832.473	3.337	-0.28	2.50	1.45e+08	
5866.451	1.067	-0.83	2.50	4.40e+08	
6091.171	2.267	-0.43	2.50	8.50e+07	
6092.792	1.887	-1.45	2.50	1.27e+08	
6098.658	3.062	-0.07	2.50	5.43e+07	
6126.216	1.067	-1.41	2.50	9.93e+06	
6599.105	0.900	-2.07	2.50	1.22e+06	
6743.122	0.900	-1.73	2.50	6.93e+05	
6745.547	2.236	-1.36	2.50	1.44e+08	

$\lambda$ [Å]	$\chi_I$ [eV]	$\log gf$	$\delta\Gamma_6$	$\Gamma_{\text{rad}}$ [s <sup>-1</sup> ]	Note	$\lambda$ [Å]	$\chi_I$ [eV]	$\log gf$	$\delta\Gamma_6$	$\Gamma_{\text{rad}}$ [s <sup>-1</sup> ]	Note	
<b>V I; <math>\log \epsilon_{\odot} = 4.00</math></b>						6200.313	2.608	-2.48	2.00	1.03e+08		
5670.853	1.081	-0.46	2.50	5.23e+06		6226.736	3.883	-2.09	2.00	5.42e+07		
5727.048	1.081	-1.22	2.50	7.57e+08		6229.228	2.845	-2.885	2.00	1.45e+08		
5727.652	1.051	-0.90	2.50	6.15e+07		6380.743	4.186	-1.366	2.00	7.34e+07		
5830.675	3.113	0.61	2.50	1.83e+08		6385.718	4.733	-1.82	2.00	2.34e+08		
6039.722	1.064	-0.72	2.50	3.98e+07		6419.950	4.733	-0.27	2.00	2.31e+08		
6090.214	1.081	-0.15	2.50	3.98e+07		6591.313	4.593	-1.99	2.00	1.40e+08		
6111.645	1.043	-0.795	2.50	3.90e+07		6608.026	2.279	-3.94	2.00	1.66e+08		
6135.361	1.051	-0.766	2.50	3.90e+07		6653.853	4.154	-2.38	2.00	2.09e+08		
6150.157	0.301	-1.54	2.50	7.81e+05		6703.567	2.758	-3.03	2.00	1.03e+08		
6199.197	0.287	-1.48	2.50	3.25e+06		6710.319	1.485	-4.79	2.00	1.66e+07		
6224.529	0.287	-1.84	2.50	1.22e+06		6726.661	4.607	-1.079	2.00	2.29e+08		
6251.827	0.287	-1.45	2.50	3.07e+07		6733.151	4.638	-1.45	2.00	2.27e+08		
6256.887	0.275	-2.17	2.50	2.94e+06		6745.101	4.580	-2.17	2.00	4.78e+07		
6452.341	1.195	-0.836	2.50	3.99e+07		6745.957	4.076	-2.74	2.00	3.79e+07		
<b>Cr I; <math>\log \epsilon_{\odot} = 5.67</math></b>						6750.153	2.424	-2.641	2.00	7.69e+06		
5628.621	3.422	-0.83	2.50	6.52e+07		6806.845	2.727	-3.11	2.00	1.02e+08		
5664.555	3.826	-0.87	2.50	4.80e+07		6810.263	4.607	-1.026	2.00	2.30e+08		
5783.886	3.322	-0.26	2.50	9.98e+07		6820.372	4.638	-1.16	2.00	2.22e+08		
5787.965	3.322	-0.21	2.50	1.00e+08		7401.685	4.186	-1.609	2.00	7.03e+07		
6630.005	1.030	-3.46	2.50	2.40e+07		7418.667	4.143	-1.476	2.00	1.06e+08		
6669.255	4.175	-0.47	2.50	3.66e+07		7421.559	4.638	-1.73	2.00	2.50e+08		
7400.226	2.900	-0.171	2.50	6.76e+07		7440.952	4.913	-0.662	2.00	4.97e+08		
<b>Cr II; <math>\log \epsilon_{\odot} = 5.67</math></b>						7443.022	4.186	-1.66	2.00	3.48e+07		
5502.067	4.168	-1.99	2.50	2.55e+07		7453.998	4.186	-2.36	2.00	1.45e+08		
<b>Fe I; <math>\log \epsilon_{\odot} = 7.51</math></b>						7498.530	4.143	-2.13	2.00	1.16e+08		
5491.832	4.186	-2.14	2.00	1.44e+08		7507.261	4.415	-0.972	2.00	9.77e+07		
5494.463	4.076	-1.85	2.00	2.90e+07		7540.430	2.727	-3.77	2.00	9.31e+07		
5522.447	4.209	-1.43	2.00	8.97e+07		7547.910	5.100	-1.247	2.00	6.38e+08		
5539.280	3.642	-2.49	2.00	2.60e+07		7551.109	5.085	-1.57	2.00	6.34e+08		
5543.936	4.217	-1.10	2.00	2.39e+08		7582.122	4.955	-1.64	2.00	1.00e+08		
5560.212	4.434	-1.09	2.00	1.64e+08		7588.305	5.033	-1.07	2.00	6.35e+08		
5577.030	5.033	-1.45	2.00	6.89e+08		7745.500	5.086	-1.149	2.00	6.37e+08		
5579.340	4.231	-2.29	2.00	2.55e+08		7746.587	5.064	-1.276	2.00	6.31e+08		
5607.664	4.154	-2.18	2.00	3.50e+08		7751.137	4.991	-0.775	2.00	6.44e+08		
5608.972	4.209	-2.31	2.00	8.89e+07		7844.559	4.835	-1.70	2.00	2.34e+08		
5611.360	3.635	-2.91	2.00	1.25e+08		<b>Fe II; <math>\log \epsilon_{\odot} = 7.51</math></b>	5823.155	5.569	-2.88	2.00	3.00e+08	not used
5618.633	4.209	-1.34	2.00	1.05e+08		6149.258	3.889	-2.84	2.00	3.39e+09		
5619.595	4.386	-1.48	2.00	1.78e+08		6247.557	3.892	-2.39	2.00	3.38e+08		
5636.696	3.640	-2.56	2.00	3.90e+07		6369.462	2.891	-4.20	2.00	2.90e+08		
5638.262	4.220	-0.88	2.00	1.94e+08		6383.722	5.553	-2.10	2.00	4.09e+08		
5646.684	4.260	-2.40	2.00	1.00e+08		6416.919	3.892	-2.69	2.00	3.37e+08	not used	
5651.469	4.473	-1.76	2.00	1.62e+08		6432.680	2.891	-3.64	2.00	2.90e+07		
5652.010	4.218	-1.82	2.00	2.36e+08		6446.410	6.223	-1.88	2.00	5.22e+08		
5741.848	4.256	-1.66	2.00	2.11e+08		6456.383	3.903	-2.24	2.00	3.37e+08		
5793.689	4.593	-1.29	2.00	5.38e+07		7449.335	3.889	-3.168	2.00	4.09e+08	not used	
5811.914	4.143	-2.38	2.00	3.76e+07		7515.831	3.903	-3.462	2.00	4.09e+08		
5814.807	4.283	-1.84	2.00	2.11e+08		<b>Co I; <math>\log \epsilon_{\odot} = 4.92</math></b>	5647.234	2.280	-1.58	2.50	1.66e+08	
5852.219	4.548	-1.21	2.00	1.90e+08		6086.658	3.409	0.22	2.50	8.87e+07		
5855.077	4.608	-1.54	2.00	1.91e+08		6093.143	1.740	-2.37	2.50	2.08e+07		
6034.035	4.312	-2.30	2.00	1.59e+08		6188.996	1.710	-2.33	2.50	2.22e+07		
6089.580	4.580	-1.30	2.00	9.27e+07		6257.572	3.713	-1.08	2.50	6.89e+07		
6094.374	4.652	-1.58	2.00	1.92e+08		6429.906	2.137	-2.39	2.50	9.29e+05		
6096.665	3.984	-1.81	2.00	4.53e+07		6632.433	2.280	-1.87	2.50	6.46e+06		
6105.131	4.548	-1.91	2.00	1.00e+08		6814.942	1.956	-1.77	2.50	2.08e+07		
6151.618	2.176	-3.329	2.00	1.55e+08		7417.367	2.042	-1.97	2.50	2.22e+07		
6157.728	4.076	-1.28	2.00	5.02e+07								
6159.378	4.607	-1.85	2.00	1.92e+08								
6165.360	4.143	-1.524	2.00	8.77e+07								
6173.336	2.223	-2.910	2.00	1.67e+08								
6187.990	3.943	-1.65	2.00	4.60e+07								

$\lambda$ [Å]	$\chi_l$ [eV]	$\log gf$	$\delta\Gamma_6$	$\Gamma_{\text{rad}}$ [s <sup>-1</sup> ]	Note
<b>Ni I; <math>\log \epsilon_{\odot} = 6.25</math></b>					
5494.876	4.105	-1.08	2.50	2.05e+08	
5578.711	1.676	-2.68	2.50	5.43e+07	
5628.335	4.089	-1.35	2.50	2.52e+08	
5638.745	3.898	-1.72	2.50	1.27e+08	
5643.072	4.165	-1.22	2.50	9.14e+07	
6025.751	4.236	-1.69	2.50	1.92e+08	
6039.296	4.236	-2.07	2.50	2.16e+08	
6086.276	4.266	-0.51	2.50	2.54e+08	
6108.107	1.676	-2.56	2.50	4.86e+07	
6111.066	4.088	-0.86	2.50	1.46e+08	
6128.963	1.676	-3.37	2.50	1.21e+07	
6130.130	4.266	-0.963	2.50	2.78e+08	
6133.963	4.088	-1.79	2.50	1.45e+08	
6176.807	4.088	-0.27	2.50	1.45e+08	
6177.236	1.826	-3.562	2.50	4.31e+07	
6186.709	4.105	-0.922	2.50	2.06e+09	
6204.600	4.088	-1.146	2.50	1.75e+08	
6370.341	3.542	-1.957	2.50	1.48e+08	
6378.247	4.154	-0.84	2.50	2.08e+08	
6424.847	4.167	-1.354	2.50	2.13e+08	
6586.308	1.951	-2.748	2.50	4.30e+07	
6598.593	4.236	-0.94	2.50	1.92e+08	
6643.629	1.676	-2.08	2.50	1.01e+08	
6767.768	1.826	-2.24	2.50	1.03e+08	
6772.313	3.658	-1.082	2.50	1.50e+08	
7414.500	1.986	-2.22	2.50	1.03e+08	
7522.758	3.658	-0.535	2.50	1.50e+08	
7525.111	3.635	-0.64	2.50	1.19e+08	
7574.043	3.833	-0.533	2.50	9.12e+07	
7826.766	3.699	-1.856	2.50	5.98e+07	